Biochemistry (Moscow), Vol. 67, No. 2, 2002, pp. 265-276. Translated from Biokhimiya, Vol. 67, No. 2, 2002, pp. 318-331.

New Structures of the O-Specific Polysaccharides of Bacteria of the Genus *Proteus*. 1. Phosphate-Containing Polysaccharides

F. V. Toukach[1], A. N. Kondakova[1], N. P. Arbatsky[1], S. N. Senchenkova[1], A. S. Shashkov[1], Y. A. Knirel[1]*, K. Zych[2], A. Rozalski[2], and Z. Sidorczyk[2]

[1]Zelinsky Institute of Organic Chemistry, Russian Academy of Sciences, Leninskii pr. 47, Moscow, 119991 Russia; fax: (095) 135-5328; E-mail: knirel@ioc.ac.ru
[2]Institute of Microbiology and Immunology, University of Lodz, Banacha 12/16, 90-237 Lodz, Poland; fax: (48-42) 678-4932; E-mail: zsidor@biol.uni.lodz.pl

Received March 23, 2001

Abstract—The O-specific polysaccharide chains (O-antigens) of the lipopolysaccharides of five *Proteus* strains, *P. vulgaris* O17, *P. mirabilis* O16 and O33, and *P. penneri* 31 and 103, were found to contain phosphate groups that link the non sugar components, e.g., ethanolamine and ribitol. The polysaccharides of *P. mirabilis* O16 and *P. penneri* 103 include ribitol phosphate in the main chain and thus resemble ribitol teichoic acids of Gram-positive bacteria. The structures of the polysaccharides were elucidated using NMR spectroscopy, including two-dimensional $^{1}H,^{1}H$ correlation spectroscopy (COSY and TOCSY), nuclear Overhauser effect spectroscopy (NOESY or ROESY), and H-detected $^{1}H,^{13}C$ and $^{1}H,^{31}P$ heteronuclear multiple-quantum coherence spectroscopy (HMQC), along with chemical methods. The structures determined are unique among the bacterial polysaccharides and, together with the data obtained earlier, represent the chemical basic for classification of *Proteus* strains. Based on structural similarities of the O-specific polysaccharides and serological relationships between the O-antigens, we propose to extend *Proteus* serogroups O17 and O19 by including *P. penneri* strains 16 and 31, respectively.

Key words: lipopolysaccharide, O-specific polysaccharide, O-antigen, bacterial polysaccharide structure, ethanolamine phosphate, ribitol phosphate, *Proteus*, NMR spectroscopy

Three bacterial species of the genus *Proteus*, *P. mirabilis*, *P. vulgaris* and *P. penneri*, commonly cause urinary tract infections that can lead to severe complications, such as acute or chronic pyelonephritis and formation of bladder and kidney stones. Currently, strains of *P. mirabilis* and *P. vulgaris* are classified into 60 O-serogroups [1, 2], and a number of new O-serogroups are proposed for non-classified strains of *P. penneri* [3, 4]. The serological O-specificity of *Proteus* is defined by the structure of the polysaccharide chain (O-antigen) of the outer-membrane lipopolysaccharide. Our chemical and immunochemical studies of the O-antigens aim at creation of the molecular basis for serological classification of *Proteus* strains.

In most *Proteus* strains studied so far, the O-specific polysaccharides contain acidic or both acidic and basic components, such as uronic acids, their amides with amino acids, ether-linked lactic acid, acetal-linked pyruvic acid, and phosphate groups [3]. We now report determination of structures of five new *Proteus* polysaccharides from three strains belonging to *P. mirabilis* serogroups O16, O17, and O33, and two unclassified strains, *P. penneri* 31 and 103.

Abbreviations: 2D) two-dimensional; COSY) correlation spectroscopy; Etn-*P*) ethanolamine phosphate; FucNAc) 2-acetamido-2,6-dideoxygalactose; Fuc3NHb) 3,6-dideoxy-3-[(R)-3-hydroxybutyramido]galactose; GLC) gas-liquid chromatography; GlcA) glucuronic acid; Hb) 3-hydroxybutyryl group; HMBC) heteronuclear multiple-bond correlation; HMQC) heteronuclear multiple-quantum coherence; NOESY) nuclear Overhauser effect spectroscopy; Rib-ol) ribitol; ROESY) rotating-frame nuclear Overhauser effect spectroscopy; TOCSY) total correlation spectroscopy.

* To whom correspondence should be addressed.

MATERIALS AND METHODS

Bacterial strains, growth, isolation of lipopolysaccharides and O-specific polysaccharides. Strains of *P. penneri* were from the Collection of the Institute of Microbiology and Immunology (University of Lodz, Poland), and

0006-2979/02/6702-0265$27.00 ©2002 MAIK "Nauka/Interperiodica"

strains of *P. vulgaris* and *P. mirabilis* came from the Czech National Collection of Type Cultures (CNCTC, Institute of Epidemiology and Microbiology, Prague, Czech Republic). The bacteria were grown on nutrient broth (Warsaw Laboratory of Sera and Vaccines) supplemented with 1% glucose. Bacterial cells were separated by centrifugation, washed with distilled water, and lyophilized.

Lipopolysaccharides were isolated by extraction of dried cells with hot aqueous phenol [5] and purified by treatment with cold aqueous 50% CCl_3CO_2H followed by dialysis of the supernatant. The lipopolysaccharides were degraded with 2% acetic acid at 100°C until the precipitation of lipid. High-molecular-mass O-specific polysaccharides were isolated from the water-soluble portion by gel-permeation chromatography on Sephadex G-50 in pyridinium–acetate buffer, pH 4.5, using a Knauer differential refractometer (Germany) for monitoring.

NMR spectroscopy. Prior to measurement, samples were deuterium-exchanged by freeze-drying twice from D_2O. NMR spectra were recorded on a Bruker DRX-500 spectrometer (Germany) equipped with a SGI INDY computer workstation for solutions in 99.96% D_2O at 30-60°C. Acetone (δ_H 2.225 ppm, δ_C 31.45 ppm) and aqueous 85% H_3PO_4 (δ_P 0 ppm) were used as internal or external standard, respectively. The parameters used for 2D experiments were essentially the same as described previously [6].

The ^1H- and ^{13}C-NMR spectra were assigned using 2D $^1H,^1H$ and $^1H,^{13}C$ shift-correlated NMR experiments and published chemical shift data for monosaccharides [7-9]. In correlation spectroscopy (COSY), cross-peaks for coupled protons were observed, whereas total correlation spectroscopy (TOCSY) revealed connectivities between all protons within each isolated spin system of sugar and ribitol residues. The spin systems of sugars and ribitol were assigned based on coupling constant values, which were determined from one-dimensional ^1H-NMR spectra. In case of signal coincidence, the coupling constants were estimated from the 2D NMR spectra. These data enabled identification of hexuronic acid residues, differentiation between sugars with the gluco- and galacto-configurations, and determination of the anomeric configuration and the pyranose form of the monosaccharides. 2D H-detected $^1H,^{13}C$ heteronuclear multiple-quantum coherence (HMQC) spectra revealed correlations between carbons and the attached protons. Amino sugars were distinguished by correlation of protons at nitrogen-bearing carbons (H2) to the corresponding carbons (C2) in the region δ_C 49-57 ppm.

Nuclear Overhauser effect spectroscopy (NOESY) and rotating-frame nuclear Overhauser effect spectroscopy (ROESY), along with typical intra-residue correlations, showed cross-peaks between each anomeric proton of the glycon and a proton at the linkage carbon of the aglycon. These data enabled determination of the linkage positions and the sequence of the sugar residues in the repeating unit. In some cases, an $^1H,^{13}C$ heteronuclear multiple-bond correlation (HMBC) experiment was used for sequence analysis, which revealed correlations between carbons and protons separated by two or three bonds. A 2D H-detected $^1H,^{31}P$ HMQC experiment was applied for determination of the location of phosphate groups.

Chemical methods. For sugar analysis, the polysaccharides were hydrolyzed with 2 M trifluoroacetic acid (120°C, 2 h), and the monosaccharides were converted into the alditol acetates [10] and analyzed by GLC on a Hewlett-Packard 5880 chromatograph (USA) equipped with a DB-5 capillary column, using a temperature gradient of 160°C (1 min) to 250°C at 3°C/min. Ribitol was identified by GLC as the O-acetylated derivative obtained after hydrolysis of the dephosphorylated polysaccharides. For identification of hexuronic acids, methanolysis of the polysaccharides was performed with 1 M hydrogen chloride in methanol and followed by acetylation with acetanhydride in pyridine (100°C, 1 h) and GLC analysis.

The absolute configurations of the monosaccharides were determined by GLC of the acetylated glycosides with (R)-2-octanol [11]. For this purpose, a portion of the methanolysate was subjected to N-acetylation followed by (R)-2-octanolysis in the presence of anhydrous CF_3COOH (120°C, 16 h) and then acetylated with acetanhydride in pyridine (100°C, 1 h). The acetylated (R)-2-octyl glycosides were analyzed by GLC and GLC/mass spectrometry on a Hewlett Packard 5890 chromatograph equipped with a Nermag R10-10L mass spectrometer (France). The chromatographic conditions were the same as in sugar analysis. The absolute configuration of ribitol in the polysaccharides of *P. mirabilis* O16 and *P. penneri* 103 was determined by periodate oxidation followed by bromine oxidation, acid hydrolysis, and GLC of the acetylated (S)-2-butyl D-glycerates derived. The absolute configuration of ribitol in the polysaccharide of *P. mirabilis* O33 was determined by oxidation with 2,2,6,6-tetramethyl-1-piperidinyloxy radical (TEMPO) [12] followed by hydrolysis (1 M trifluoroacetic acid, 100°C, 30 min), dephosphorylation with aqueous 48% HF and GLC analysis of the acetylated (R)-2-octyl ester of D-ribonic acid derived.

Dephosphorylation of the polysaccharides was performed with aqueous 48% HF (0.2 ml, 5°C, 24 h), and the products were isolated by gel-permeation chromatography on Sephadex G-25 in water.

RESULTS

***Proteus penneri* strain 31.** Sugar analysis revealed D-Gal, D-GlcN, D-GalN, and L-FucN as components of the polysaccharide repeating unit.

The ^1H- and ^{13}C-NMR (Fig. 1) spectra showed that the polysaccharide is regular and has a tetrasaccharide repeating unit (there were signals for four anomeric atoms

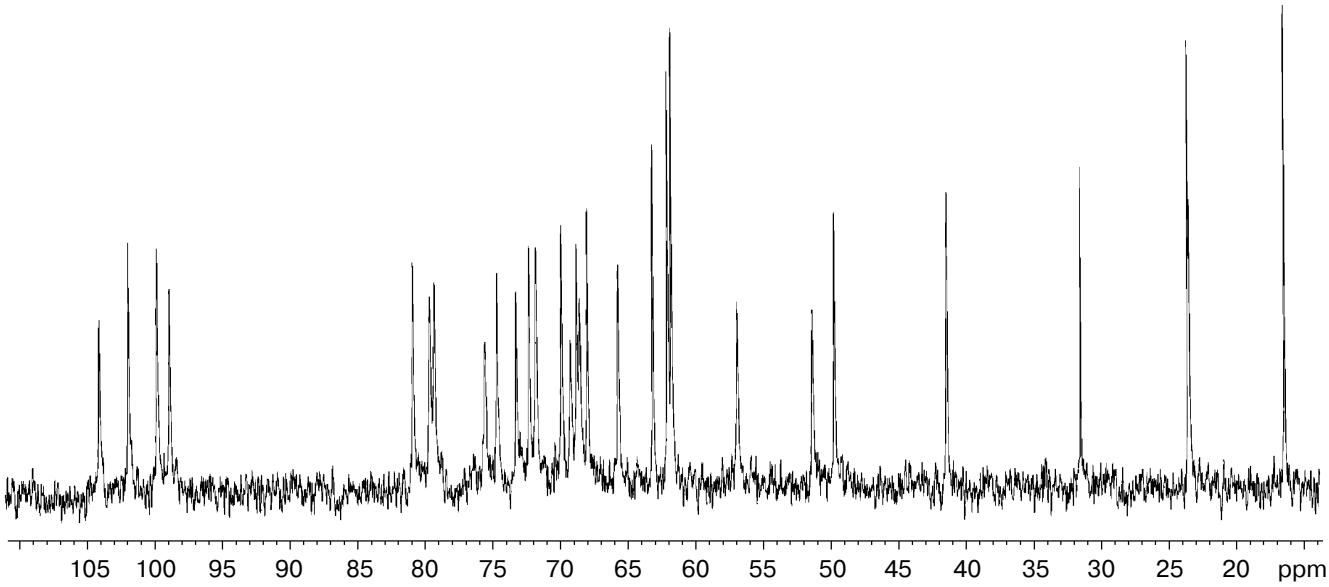

Fig. 1. ^{13}C-NMR spectrum of the O-specific polysaccharide of *P. penneri* 31 (the region of CO resonances is not shown).

at δ_H 4.67, 4.93, 5.01, 5.12 ppm and δ_C 98.7, 99.6, 101.8, 103.9 ppm). The repeating unit contains three N-acetylamino sugars (signals for carbons linked to nitrogen at δ 49.6, 51.2, 56.8 ppm, and for N-acetyl groups at δ_H 1.96, 1.98, 2.03 ppm and δ_C 23.4-23.5 ppm (CH_3), 174.8-175.3 ppm (CO)), one 6-deoxy sugar (CH_3 at δ_H 1.19 ppm and δ_C 16.2 ppm), and ethanolamine (CH_2O at δ_C 62.1 ppm; CH_2N at δ_H 3.28 ppm and δ_C 41.5 ppm). In the ^{31}P-NMR spectrum, a signal for a monophosphate group was observed at δ 3.2 ppm.

The ^{1}H- and ^{13}C-NMR spectra were assigned using two-dimensional shift-correlated spectroscopy, and the chemical shift data are tabulated in Tables 1 and 2. The sugar residues were identified as Glc*p*NAc ($J_{3,4}$ and $J_{4,5}$ ~ 10 Hz), Gal*p*NAc, Fuc*p*NAc, and Gal*p* ($J_{3,4}$ and $J_{4,5} \leq$ 3 Hz). Fuc*p*NAc was recognized by a H5/H6 correlation at δ 4.42/1.19 ppm in the COSY spectrum and a H5/H4 correlation at δ 4.42/3.91 ppm in the ROESY spectrum.

A large $J_{1,2}$ coupling constant value of ~7 Hz determined for Glc*p*NAc is typical of a β-linked sugar. The anomeric signals for the other sugar residues were not resolved, and this, together with their relatively low-field position at δ 4.93-5.12 ppm, suggested that they are α-linked. These conclusions were confirmed by a ROESY experiment, which revealed H1/H3 and H1/H5 correlations typical of β-linked sugars only for Glc*p*NAc residue, whereas H1/H2 correlations that are typical of α-linked sugars, were observed for three other sugar residues.

The ^{1}H,^{31}P HMQC spectrum showed correlations of the ^{31}P-NMR signal with the proton signals of the ethanolamine residue at δ 3.2/3.28 ppm (CH_2N) and δ 3.2/4.12 ppm (CH_2O), as well as with the H6 signal of Glc*p*NAc at δ 3.2/4.17 ppm. These data indicated that the ethanolamine phosphate group (Etn-*P*) is attached to O6 of Glc*p*NAc, which is in agreement with a low-field position of the C6 signal at δ 65.5 ppm compared to its position at δ 61.9 ppm in the unsubstituted monosaccharide [8] (α-effect of phosphorylation).

A low-field displacement (α-effect of glycosylation) of the signals for C3 of Fuc*p*NAc to δ 74.4 (+5.7 ppm) and Gal*p* to δ 80.7 (+10.6 ppm), C3 and C6 of Glc*p*NAc to δ 79.0 and 65.5 (+4.2 and +3.7 ppm, respectively), and C4 of Gal*p*NAc to δ 79.4 (+9.9 ppm), as compared with the data of the corresponding nonsubstituted monosaccharides [8], revealed the glycosylation pattern in the repeating unit.

In addition to intraresidue cross-peaks, the ROESY spectrum contained cross-peaks for the following transglycosidic protons: Gal*p* H1/Gal*p*NAc H4, Gal*p*NAc H1/Fuc*p*NAc H3, Fuc*p*NAc H1/Glc*p*NAc H3, and Glc*p*NAc H1/Gal*p* H3 at δ 4.93/4.09, 5.12/4.02, 5.01/3.73, and 4.67/3.95 ppm, respectively. These data showed that the polysaccharide has a tetrasaccharide repeating unit having the structure that is shown in Table 3.

***Proteus vulgaris* O17.** Sugar analysis showed that the polysaccharide contained D-Glc, D-GlcN, D-GlcA, and D-Fuc3N. The last sugar was identified by comparison with the authentic sample from the O-specific polysaccharide of *Proteus penneri* 16 studied earlier [13], and its D-configuration was determined by analysis of the effects of glycosylation in the ^{13}C-NMR spectrum (see below). As in chemical studies of the *P. penneri* 16 polysaccharide [13], part of this sugar was detected by GLC/MS as the N-(3-hydroxybutyryl) derivative owing to incomplete hydrolysis of the amidic bond, whereas the

Table 1. ^{1}H-NMR data (δ, ppm)

Residue	H1(1a)	H2	H3	H4	H5(5a)	H6a(5b)	H6b
P. penneri 31 polysaccharide							
→3)-α-Gal*p*-(1→	4.93	3.90	3.95	4.23	4.03	3.82	3.89
→4)-α-Gal*p*NAc-(1→	5.12	4.21	4.01	4.09	4.29	3.64	3.71
→3)-α-Fuc*p*NAc-(1→	5.01	4.32	4.02	3.91	4.42	1.19	
→3)-β-Glc*p*NAc-(1→	4.67	3.92	3.73	3.64	3.58	4.17	4.17
Etn-*P*-(O→	4.12	3.28					
P. vulgaris O17 dephosphorylated polysaccharide							
→3)-α-Glc*p*NAc-(1→	5.41	4.11	3.59	3.52	3.61	3.78	3.85
→2)-β-Fuc*p*3N-(1→	4.61	3.65	4.14	3.65	3.86	1.24	
→6)-α-Glc*p*-(1→	5.47	3.44	3.66	3.27	3.80	3.78	4.08
→4)-β-Glc*p*A-(1→	4.40	3.36	3.75	3.82	3.75		
Hb		2.44	4.19	1.22			
P. vulgaris O17 polysaccharide[a]							
→3)-α-Glc*p*NAc-(1→	5.41	4.13	3.62	3.62	3.75	4.07	4.15
	(5.50)			(3.54)	(3.75)	(3.77)	(3.87)
→2)-β-Fuc*p*3N-(1→	4.62	3.64	4.14	3.66	3.87	1.25	
→6)-α-Glc*p*-(1→	5.43	3.47	3.64	3.26	3.72	3.75	4.08
	(5.49)						
→4)-β-Glc*p*A-(1→	4.48	3.38	3.77	4.03	3.77		
Hb		2.45	4.17	1.22			
Etn-*P*-(O→	4.14	3.30					
P. mirabilis O33 polysaccharide[a]							
→2)-β-Gal*p*-(1→	4.59	3.87	4.27	4.13	3.70	3.75	3.87
→3)-α-Glc*p*NAc-(1→	5.21	4.05	3.96	3.61	4.03	3.81	3.81
→3)-β-Glc*p*-(1→	4.49	3.37	3.57	3.66	3.56	4.04	4.15
	(4.51)	(3.38)	(3.57)	(3.58)	(3.56)	(3.7-3.9)	
→3)-β-Glc*p*NAc-(1→	4.91	3.87	3.71	3.45	3.43	3.70	3.90
Rib-ol-5-*P*-(O→	3.64[c]	3.84	3.73	3.94	4.03	4.13	
Etn-*P*-(O→	4.10	3.26					
P. penneri 103 polysaccharide							
→4)-β-Glc*p*-(1→	4.68	3.43	3.70	3.94	3.71	3.99	4.24
→3)-β-Gal*p*-(1→	4.51	3.67	3.77	4.20	3.66	3.70-3.81	
→3)-β-Gal*p*NAc-(1→	4.71	4.05	3.88	4.15	3.70	3.70-3.81	
→4)-Rib-ol-5-*P*-(O→	3.63[b]	3.82	3.82	4.13	3.99	4.18	
Etn-*P*-(O→	4.11	3.28					
Oligosaccharide from *P. mirabilis* O16 polysaccharide							
β-Gal*p*NAc-(1→	4.69	3.92	3.77	3.93	3.67	3.80	3.80
→4)-α-Gal*p*NAc-(1→	5.36	4.14	3.92	4.18	3.87	3.79	3.92
→3)-α-Glc*p*NAc-(1→	5.11	4.05	3.89	3.69	3.80	3.71	3.85
→2)-Rib-ol	3.83[d]	3.96	3.91	3.75	3.64	3.81	
P. mirabilis O16 polysaccharide[a]							
→6)-β-Gal*p*NAc-(1→	4.71	3.92	3.77	3.98	3.83	4.05	4.06
→4)-α-Gal*p*NAc-(1→	5.34	4.13	3.92	4.19	3.87	3.81	3.90
	(5.35)						
→3)-α-Glc*p*NAc-(1→	5.10	4.06	3.93	3.75	4.14	4.12	4.18
	(5.09)	(4.04)	(3.92)	(3.69)	(3.81)	(3.72)	(3.86)
→2)-Rib-ol-5-*P*-(O→	3.82[d]	3.98	3.93	3.83	3.97	4.06	
Etn-*P*-(O→	4.14	3.29					

Note: Chemical shifts for NAc groups are δ 1.96-2.07 ppm.

[a] When different, chemical shifts for repeating units lacking Etn-*P* are given in parentheses.

[b] H1b at δ 3.81 ppm.

[c] H1b at δ 3.79 ppm.

[d] H1b at δ 3.90 ppm.

Table 2. ^{13}C-NMR data (δ, ppm)

Residue	C1	C2	C3	C4	C5	C6
P. penneri 31 polysaccharide						
→3)-α-Gal*p*-(1→	101.8	68.6	80.7	69.7	73.0	61.9
→4)-α-Gal*p*NAc-(1→	99.6	51.2	68.3	79.4	71.9	61.6
→3)-α-Fuc*p*NAc-(1→	98.7	49.6	74.4	72.1	67.8	16.2
→3)-β-Glc*p*NAc-(1→	103.9	56.8	79.0	69.0	75.4	65.5
Etn-*P*-(O→	62.1	41.5				
P. vulgaris O17 dephosphorylated polysaccharide						
→3)-α-Glc*p*NAc-(1→	96.8	53.0	82.4	69.6	73.7	62.0
→2)-β-Fuc*p*3N-(1→	104.9	72.0	54.1	72.0	73.2	16.5
→6)-α-Glc*p*-(1→	99.1	72.9	74.2	71.0	71.4	68.8
→4)-β-Glc*p*A-(1→	104.2	74.1	77.5	77.3	77.1	175.1
Hb	175.1	46.1	66.1	23.7		
P. vulgaris O17 initial polysaccharide[a]						
→3)-α-Glc*p*NAc-(1→	97.2	53.0	82.0	69.3	72.7	65.8
	(97.0)		(82.1)	(69.7)	(73.4)	(62.2)
→2)-β-Fuc*p*3N-(1→	105.0	72.7	54.1	71.9	73.4	16.5
→6)-α-Glc*p*-(1→	99.8	72.3	74.0	71.3	71.8	69.3
	(99.5)			(71.1)		
→4)-β-Glc*p*A-(1→	104.2	73.8	77.6	75.8	77.3	175.1
				(75.4)		
Hb	174.0	46.1	66.2	23.7		
Etn-*P*-(O→	62.2	41.5				
P. mirabilis O33 polysaccharide[a]						
→2)-β-Gal*p*-(1→	101.9	76.6	79.9	68.9	75.9	62.0
→3)-α-Glc*p*NAc-(1→	99.2	53.6	81.6	69.7	72.8	61.8
→3)-β-Glc*p*-(1→	104.7	73.1	83.5	70.7	75.8	65.5
	(104.5)			(71.1)		(62.2)
→3)-β-Glc*p*NAc-(1→	101.5	55.3	86.1	70.3	76.8	62.4
Rib-ol-5-*P*-(O→	63.8	73.5	73.1	72.3	67.9	
Etn-*P*-(O→	63.2	41.4				
P. penneri 103 polysaccharide						
→4)-β-Glc*p*-(1→	104.0	74.0	75.9	74.9	74.6	65.7
→3)-β-Gal*p*-(1→	105.0	70.6	83.3	68.7	75.5	61.8[b]
→3)-β-Gal*p*NAc-(1→	102.1	52.1	80.7	68.8	75.5	61.7[b]
→4)-Rib-ol-5-*P*-(O→	63.5	72.5[c]	72.6[c]	80.1	66.3	
Etn-*P*-(O→	62.5	41.0				
Oligosaccharide from *P. mirabilis* O16 polysaccharide						
β-Gal*p*NAc-(1→	103.5	54.0	72.3	69.2	76.2	62.3
→4)-α-Gal*p*NAc-(1→	99.1	51.2	69.1	76.5	71.6	61.3
→3)-α-Glc*p*NAc-(1→	98.8	53.6	78.0	72.2	73.7	61.6
→2)-Rib-ol	61.1	80.8	73.5	72.7	64.1	
P. mirabilis O16 polysaccharide[a]						
β-Gal*p*NAc-(1→	103.5	54.0	72.2	68.8	74.8	65.6
→4)-α-Gal*p*NAc-(1→	99.1	51.2	69.0	76.6	71.6	61.6
	(99.0)			(76.5)		
→3)-α-Glc*p*NAc-(1→	99.3	53.6	77.9	71.5	72.5	65.3
	(99.2)		(78.0)	(72.1)	(73.6)	(61.5)
→2)-Rib-ol-5-*P*-(O→	61.2	81.4	73.0	71.6	68.2	
	(61.1)	(81.2)	(72.9)		(68.1)	
Etn-*P*-(O→	63.1	41.3				

Note: Chemical shifts for NAc groups are δ 23.2-23.7 ppm (CH_3) and 175.1-176.3 ppm (CO).

[a] When different, chemical shifts for repeating units lacking Etn-*P* are given in parentheses.

[b,c] Assignment could be interchanged.

Table 3. Structures of the new phosphorylated O-specific polysaccharides and structurally related O-specific polysaccharides of *Proteus*

Proteus strain	Structure of the O-specific polysaccharide
Proteus penneri 31	Etn-*P* (6) → →3)-α-D-Gal*p*-(1→4)-α-D-Gal*p*NAc-(1→3)-α-L-Fuc*p*NAc-(1→3)-β-D-Glc*p*NAc-(1→
Proteus vulgaris O17	~60% Etn-*P* (6) → →3)-α-D-Glc*p*NAc-(1→2)-β-D-Fuc*p*3NHb-(1→6)-α-D-Glc*p*-(1→4)-β-D-Glc*p*A-(1→
Proteus mirabilis O33 (= *Proteus mirabilis* D52 [17])	D-Rib-ol-5-*P* (3); ~75% Etn-*P* (6) → →2)-β-D-Gal*p*-(1→3)-α-D-Glc*p*NAc-(1→3)-β-D-Glc*p*-(1→3)-β-D-Glc*p*NAc-(1→
Proteus penneri 103	Etn-*P* (6) → →4)-β-D-Glc*p*-(1→3)-β-D-Gal*p*-(1→3)-β-D-Gal*p*NAc-(1→4)-D-Rib-ol-5-*P*-(O→
Proteus mirabilis O16	~65% Etn-*P* (6) → →6)-β-D-Gal*p*NAc-(1→4)-α-D-Gal*p*NAc-(1→3)-α-D-Glc*p*NAc-(1→2)-D-Rib-ol-5-*P*-(O→
Proteus vulgaris O19 [21]	→3)-α-D-Gal*p*-(1→4)-α-D-Gal*p*NAc-(1→3)-α-L-Fuc*p*NAc-(1→3)-β-D-Glc*p*NAc-(1→
Proteus penneri 16 [13]	α-D-Glc*p* (1→2) → →3)-α-D-Glc*p*NAc-(1→2)-β-D-Fuc*p*3NHb-(1→6)-α-D-Glc*p*-(1→4)-β-D-Glc*p*A-(1→
Proteus penneri 63 [22]	β-D-Glc*p* (1→4); Etn-*P* (6) → →6)-α-D-Glc*p*NAc-(1→3)-α-L-Fuc*p*NAc-(1→3)-β-D-Glc*p*NAc-(1→2)-β-D-Glc*p*-(1→

other part, as well as GlcN, was present as the N-acetyl derivative.

As judged by the ^{1}H- and ^{13}C-NMR spectra, the initial O-specific polysaccharide lacked strict regularity. The presence of the signals for ethanolamine (CH_2O at δ_C 62.2 ppm; CH_2N at δ_H 3.30 and δ_C 41.5 ppm) and phosphate (δ_P 2.06 ppm) enabled suggestion that irregularity was due to non-stoichiometric phosphorylation with ethanolamine phosphate (Etn-*P*). Indeed, the NMR spectra of the dephosphorylated polysaccharide were typical of a regular polymer. The ^{13}C-NMR spectrum (Fig. 2) contained signals for four anomeric carbons at δ 96.8, 99.1, 104.2, and 104.9 ppm, one nonsubstituted (δ 62.0 ppm) and one substituted (δ 68.8 ppm) $HOCH_2$-groups (data of the DEPT-135 spectrum), one CH_3-group of a 6-deoxy sugar at δ 16.5 ppm, two nitrogen-bearing carbons at δ 53.0 and 54.1 ppm, two N-acetyl groups (CH_3 at δ 23.5 and 23.7 ppm, CO at δ 175.1 ppm), and one 3-hydroxybutyryl group (Hb) (CH_3, CH_2, and CHOH at δ 23.7, 46.1, and 66.1 ppm, respectively). Accordingly, the ^{1}H-NMR spectrum of the polysaccharide contained, *inter alia*, signals for four anomeric protons at δ 4.40-5.47 ppm, two N-acetyl groups at δ 2.02 ppm (6H) and Hb at δ 1.24 ppm (CH_3) and 2.44 ppm (CH_2). Therefore, the dephosphorylated polysaccharide has a tetrasaccharide repeating unit.

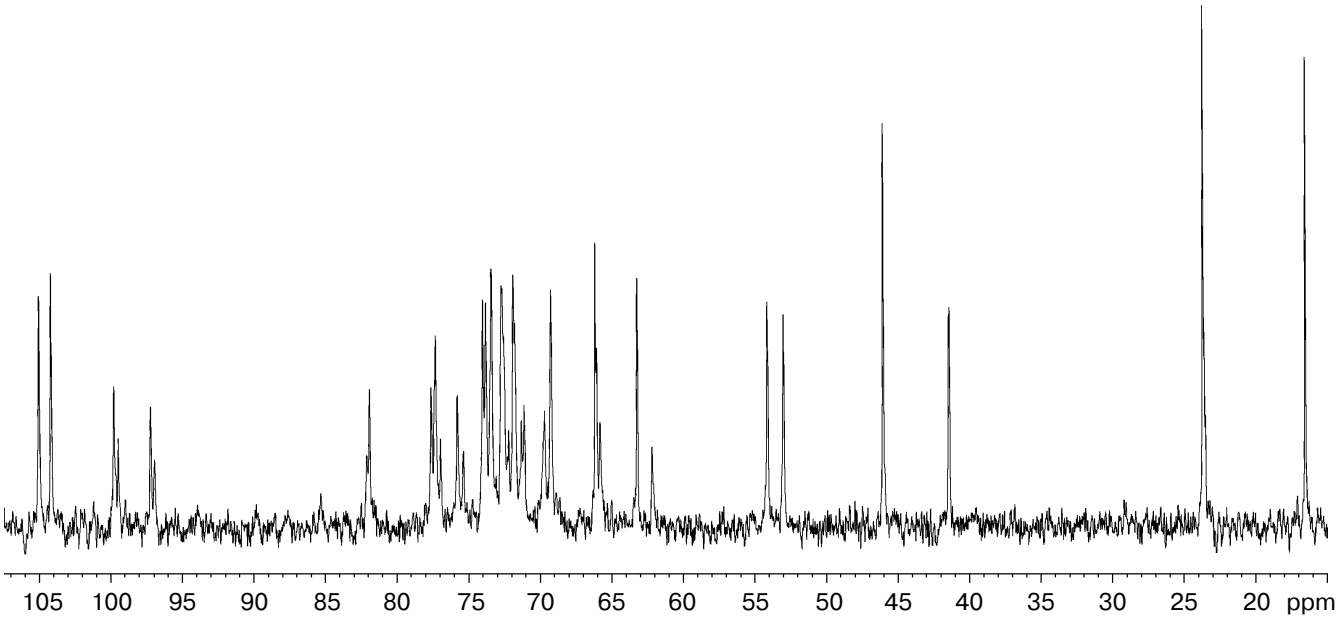

Fig. 2. ^{13}C-NMR spectrum of the dephosphorylated O-specific polysaccharide of *P. vulgaris* O17 (the region of CO resonances is not shown).

The ^{1}H- and ^{13}C-NMR spectra of the polysaccharide were assigned using 2D NMR experiments, and their chemical shifts are summarized in Tables 1 and 2. It was found that all monosaccharides in the repeating unit are present in the pyranose form, and they were identified as described for the polysaccharide of *P. penneri* 31 (see above). As judged by relatively large $^{3}J_{1,2}$ coupling constants values of 7.5 Hz determined from the ^{1}H-NMR spectrum for the anomeric protons at δ 4.40 and 4.61 ppm, the residues of Glc*p*A and Fuc*p*3NHb are β-linked, whereas the values of 3.0-3.5 Hz for Glc*p*NAc and Glc*p* showed that these sugars are α-linked. These findings were confirmed by a ROESY experiment, which revealed intraresidue H1/H3 and H1/H5 correlations that are typical of β-sugars, only for residues of Glc*p*A and Fuc*p*3NHb.

The ROESY experiment revealed also the following interresidue correlations: Fuc*p*3NHb H1/Glc*p* H6a,H6b; Glc*p* H1/Glc*p*A H4; Glc*p*A H1/Glc*p*NAc H3, and Glc*p*NAc H1/Fuc*p*3NHb H2 at δ 4.61/3.78, 4.08; 5.47/3.82; 4.40/3.59, and 5.41/3.65 ppm, respectively. The signals for H2 and H4 of Fuc*p*3NHb coincided, but a Glc*p*NAc H1/Fuc*p*3NHb H1 cross-peak at δ 5.41/4.61 ppm showed that Fuc*p*3NHb is substituted by Glc*p*NAc at position 2.

A low-field displacement of the signals for C4 of Glc*p*A to δ 77.3 (+5.0 ppm), C3 of Glc*p*NAc to δ 82.4 (+10.4 ppm), and C6 of Glc*p* to δ 68.8 (+6.9 ppm), as compared with their positions in the corresponding non-subsituted monosaccharides [8], confirmed the glycosylation pattern and the linear character of the polysaccharide. A small substitution effect on the C1 chemical shift of Glc*p*NAc (+4.9 ppm) indicated that Glc*p*NAc and Fuc*p*3NHb have the same absolute configuration and, hence, D-Fuc*p*3NHb is present in the polysaccharide (an effect of +7 ppm would be observed in case of different configurations [14]).

The data obtained demonstrated the following structure of the repeating unit of the dephosphorylated polysaccharide:

→3)-α-D-Glc*p*NAc-(1→2)-β-D-Fuc*p*3NHb-

-(1→6)-α-D-Glc*p*-(1→4)-β-D-Glc*p*A-(1→

These findings allowed also the assignment of the ^{1}H- and ^{13}C-NMR spectra of the initial polysaccharide (Tables 1 and 2) and the comparison of the chemical shifts with those of the dephosphorylated polysaccharide. The spectra of the initial polysaccharide contained minor series of signals, which resembled the corresponding spectra of the dephosphorylated polysaccharide. These signals came from the repeating units lacking Etn-*P*, whereas the major series belonged to the repeating units bearing Etn-*P* at position 6 of Glc*p*NAc. This conclusion followed from a characteristic downfield displacement of the signal for C6 from δ 62.0 ppm in the dephosphorylated polysaccharide to δ 65.8 ppm in the initial polysaccharide. Comparison of the integral intensities of the signals of the major and minor series enabled determination of the degree of phosphorylation as ~60%.

Therefore, the repeating unit of the O-specific polysaccharide of *Proteus vulgaris* O17 has the structure shown in Table 3.

***Proteus mirabilis* O33.** Chemical analyses of the polysaccharide composition showed the presence of D-Glc, D-Gal, D-GlcNAc, and D-ribitol (D-Rib-ol).

The ^{13}C-NMR spectrum of the polysaccharide (Fig. 3) contained major series of signals for a tetrasaccharide repeating unit. There were signals for anomeric carbons at δ 99.2, 101.5, 101.9, and 104.7 ppm, two sugar nitrogen-bearing carbons at δ 53.6 and 55.3 ppm, two N-acetyl groups at δ 23.8 ppm ($2CH_3$), δ 174.9 and 176.1 ppm (CO), one ethanolamine residue at δ 41.4 and 63.2 ppm, four unsubstituted (δ 61.8, 62.0, 62.4, and 63.8 ppm) and two substituted (δ 65.5 and 67.9 ppm) CH_2OH-groups, and signals for 17 other carbons linked to oxygen at δ 68.9-86.1 ppm.

Accordingly, the ^{1}H-NMR spectrum of the polysaccharide showed signals for four anomeric protons at δ 4.49-5.21 ppm, CH_2N-group of ethanolamine at δ 3.26 ppm and two N-acetyl groups at δ 2.06 and 2.07 ppm. The ^{31}P-NMR spectrum contained signals for two phosphate groups at δ 1.52 and 2.70 ppm. Therefore, it was suggested that the repeating unit of the polysaccharide contains two hexose residues (Glc*p* and Gal*p*), two residues of N-acetylated amino sugars (Glc*p*NAc), and one group each of Etn-*P* and Rib-ol-*P*.

The ^{1}H- and ^{13}C-NMR spectra were assigned using two-dimensional NMR experiments, and the chemical shifts are summarized in Tables 1 and 2. Based on the $J_{H,H}$ coupling constants values, five spin systems were assigned to one residue each of Glc*p*, Gal*p*, and Rib-ol and two residues of Glc*p*NAc.

As judged by large $J_{1,2}$ coupling constant values of 7.0-7.5 Hz determined from the ^{1}H-NMR spectrum for the anomeric protons at δ 4.49, 4.59, and 4.91 ppm, the residues of Glc*p*, Gal*p*, and one of the Glc*p*NAc residues are β-linked. The second Glc*p*NAc residue that gave a non-resolved singlet for the anomeric proton at δ 5.21 ppm, is α-linked. These conclusions were confirmed by a ROESY experiment, which revealed intraresidue H1/H5 correlations for β-Glc*p*, β-Gal*p*, and β-Glc*p*NAc but not for α-Glc*p*NAc.

A low-field displacement of the signals for C3 and C6 of Glc*p* to δ 83.5 and 65.5 (+6.5 and +3.4 ppm), C2 and C3 of Gal*p* to δ 76.6 and 79.9 (+3.4 and +5.8 ppm), C5 of Rib-ol to δ 67.9 (+4.1 ppm), C3 of α-Glc*p*NAc and β-Glc*p*NAc to δ 81.6 and 86.1 (+9.6 and +9.0 ppm, respectively), as compared with their positions in the spectra of the corresponding unsubstituted monosaccharides [8, 9], showed that the polysaccharide is linear and revealed the glycosylation pattern in the repeating unit.

The phosphorylation pattern was established using a ^{1}H,^{31}P HMQC experiment. The ^{31}P-NMR signal of Etn-*P* gave a cross-peak with H6a,Hb of Glc*p* at δ 2.70/4.04 and 2.70/4.15 ppm, thus indicating the location of ethanolamine phosphate at position 6 of Glc*p*. The other ^{31}P-NMR signal gave cross-peaks with H3 of Gal*p* at δ 1.52/4.27 ppm and H5a,5b of ribitol at δ 1.52/4.03 and δ 1.52/4.13 ppm; hence, ribitol 5-phosphate is present and attached at position 3 of Gal*p*.

The ROESY experiment revealed the following interresidue correlations between the transglycosidic protons: Gal*p* H1/α-Glc*p*NAc H3 at δ 4.59/3.96 ppm, α-Glc*p*NAc H1/Glc*p* H3 at δ 5.21/3.57 ppm, and Glc*p* H1/β-Glc*p*NAc H3 at δ 4.49/3.71 ppm. The inter-

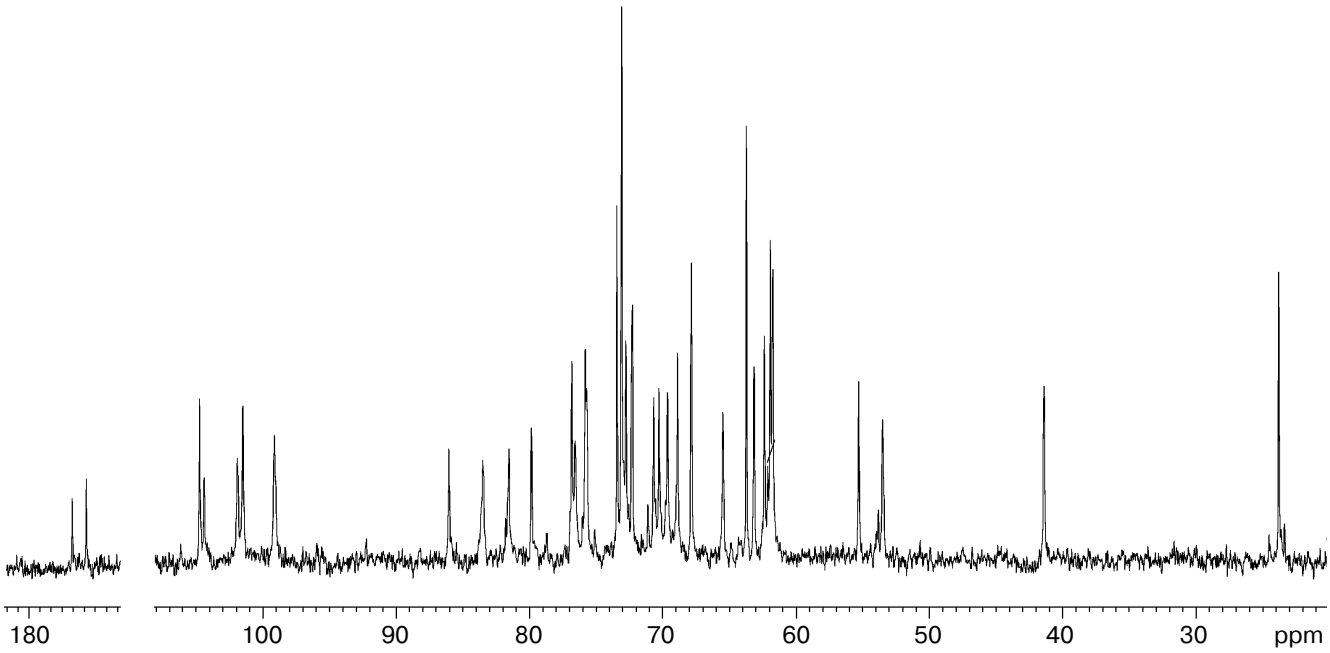

Fig. 3. ^{13}C-NMR spectrum of the O-specific polysaccharide of *P. mirabilis* O33.

residue cross-peak for β-Glc*p*NAc H1 coincided with the intraresidue β-Glc*p*NAc H1/H2 cross-peak at δ 4.91/3.87 ppm. However, taking into account the ^{13}C-NMR chemical shift data (see above), it could be inferred that β-Glc*p*NAc is attached at position 2 of Gal*p*.

Analysis of the minor signals in the NMR spectra using a 2D ^{1}H,^{13}C HMQC experiment revealed a significant difference in the position of the C6 signal of the Glc*p* residue, which appeared at δ 65.5 ppm in the major series but at δ 62.2 ppm in the minor series. Signals for C1 (δ 104.7 and 104.5 ppm) and C4 (δ 70.7 and 71.1 ppm), as well as all ^{1}H-NMR signals (Table 1) of this residue were split as well. This finding demonstrated non-stoichiometric substitution of Glc*p* with Etn-*P*. Based on the relative intensities of the signals for C1 and C6 of Glc*p* and Glc*p*6*P*Etn, the degree of phosphorylation was estimated as ~75%.

On the basis of these data, it was concluded that the O-specific polysaccharide of *P. mirabilis* O33 has the structure shown in Table 3.

***Proteus penneri* strain 103.** Sugar analyses after full acid hydrolysis of the polysaccharide revealed D-Glc, D-Gal, D-GalNAc, and D-Rib-ol.

The ^{13}C-NMR spectrum (Fig. 4) suggested that the O-specific polysaccharide is regular and has an oligosaccharide repeating unit containing one N-acetylamino sugar, two hexose residues, and one residue each of a pentitol and ethanolamine. The spectrum showed signals for three anomeric carbons at δ 102.1, 104.0, and 105.0 ppm, one carbon linked to nitrogen at δ 52.1 ppm, one N-acetyl group at δ 23.3 ppm (CH_3) and 175.7 ppm (CO), one CH_2N-group of ethanolamine at δ 41.0 ppm, six CH_2O groups at δ 61.7-66.3 ppm (C6 of three sugar residues, C1 and C5 of pentitol, and C1 of ethanolamine), and 14 other carbons linked to oxygen at δ 68.7-83.3 ppm. Accordingly, the ^{1}H-NMR spectrum contained signals for three anomeric protons at δ 4.51, 4.68, and 4.71 ppm, one residue of ethanolamine at δ 3.28 ppm (CH_2N, t, 2H), and one N-acetyl group at δ 2.07 ppm (CH_3, s, 3H). The ^{31}P-NMR spectrum contained signals for two phosphate groups at δ 1.3 and 1.7 ppm.

The ^{1}H- and ^{13}C-NMR chemical shift data of the polysaccharide are given in Tables 1 and 2. Based on typical $J_{H,H}$ coupling constants values, three sugar spin systems were assigned to Glc*p*, Gal*p*, and Gal*p*NAc. As judged by a relatively large $J_{1,2}$ coupling constant value of ~8 Hz, all three sugar residues are β-linked. This conclusion was confirmed by a ROESY experiment, which revealed intraresidue correlations between H1 and H3,H5 for all three monosaccharides, which is typical of β-pyranosides.

Low-field displacements (α-effects of glycosylation and phosphorylation) of the signals for C4 and C6 of Glc*p* to δ 74.9 and 65.7 (+4.2 and +3.9 ppm, respectively), C3 of Gal*p* to δ 83.3 (+9.5 ppm), C3 of Gal*p*NAc to δ 80.7 (+8.3 ppm), C4 and C5 of Rib-ol to δ 80.1 and 66.3 (+6.6 and +2.5 ppm, respectively) demonstrated the modes of substitution of the monosaccharides in the repeating unit.

The glycosylation pattern was confirmed and the sequence of the monosaccharides was determined by ROESY and ^{1}H,^{13}C HMBC experiments. The ROESY spectrum showed the following interresidue correlations between the transglycosidic protons: Glc*p* H1/Gal*p* H3, Gal*p* H1/Gal*p*NAc H3, and Gal*p*NAc H1/Rib-ol H4 at δ 4.68/3.77, 4.51/3.88, and 4.71/4.13 ppm, respectively. Accordingly, the HMBC spectrum revealed the following interresidue correlations: Glc*p* H1/Gal*p* C3, Gal*p* H1/Gal*p*NAc C3, and Gal*p*NAc H1/Rib-ol C4 at δ 4.68/83.3, 4.51/80.7, and 4.71/80.1 ppm, respectively.

The ^{1}H,^{31}P HMQC experiment showed a correlation of the phosphorus signal at δ 1.7 ppm with the signals for Etn at δ 4.11 ppm and H6a,H6b of Glc*p* at δ 3.99 and

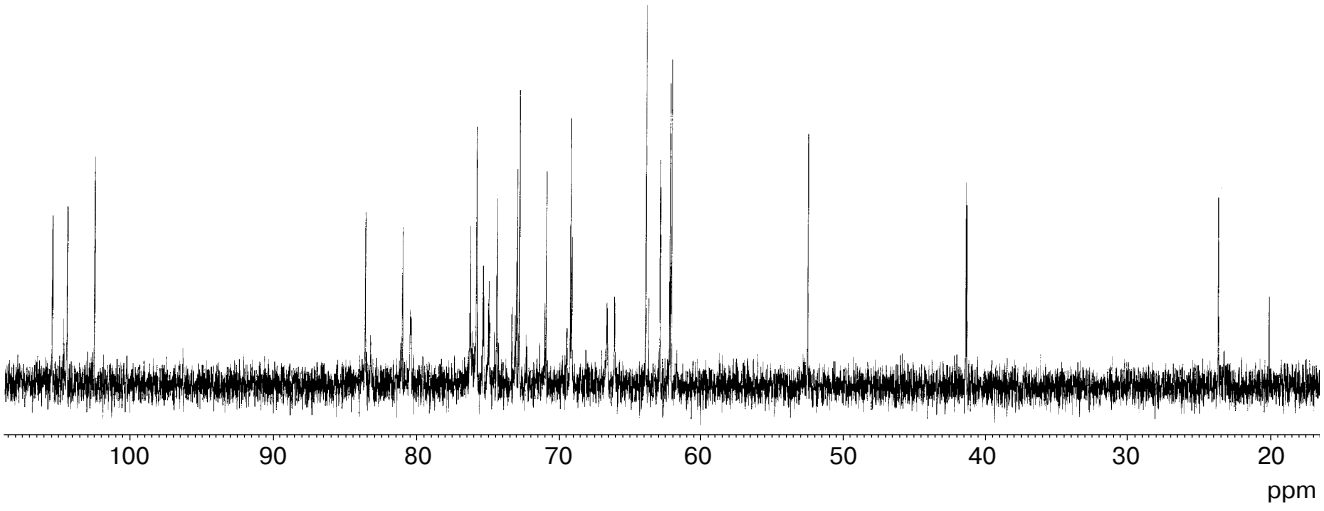

Fig. 4. ^{13}C-NMR spectrum of the O-specific polysaccharide of *P. penneri* 103 (the region of CO resonances is not shown).

4.24 ppm; hence, Etn-*P* is attached at Glc*p* at position 6. The other phosphorus signal at δ 1.3 ppm gave cross-peaks with the signals for H5a,H5b of Rib-ol at δ 3.99 and 4.18 ppm, as well as with the H4 signal of Glc*p* at δ 3.94 ppm. Therefore, ribitol and glucose residues are connected via a phosphate group. This conclusion was in agreement with splitting, due to coupling between carbon and phosphorus, of the signals for C1 and C2 of ethanolamine, C4 and C5 of ribitol, and C4-C6 of Glc*p* in the ^{13}C-NMR spectrum.

These data enabled determination of the structure of the O-specific polysaccharide of *P. penneri* 103 shown in Table 3.

***Proteus mirabilis* O16.** Sugar analysis showed that the polysaccharide contains two residues of D-GalNAc and one residue each of D-GlcNAc and D-Rib-ol.

The ^{1}H- and ^{13}C-NMR (Fig. 5) spectra of the O-specific polysaccharide showed two series of signals with the ratio of the integral intensities ~1 : 2, and it was suggested that the regularity of the polysaccharide is masked by non-stoichiometric phosphorylation with ethanolamine phosphate. The NMR spectra were too complex to be directly assigned, and, therefore, the polysaccharide was dephosphorylated with aqueous 48% hydrofluoric acid to give an oligosaccharide isolated by gel-permeation chromatography.

The ^{13}C-NMR spectrum suggested that the oligosaccharide is a trisaccharide (there were signals for three anomeric carbons at δ 99.1, 98.8, and 103.5 ppm), consisting of three N-acetylamino sugars (signals for three nitrogen-bearing carbons at δ 51.2, 53.6, and 54.0 ppm, and three N-acetyl groups at δ 23.3-23.6 ppm (CH_3) and δ 175.3-176.3 ppm (CO)) and a pentitol residue (five $HOCH_2$-groups at δ 61.1-64.1 ppm). Accordingly, the ^{1}H-NMR spectrum the oligosaccharide contained signals for three anomeric protons at δ 4.69, 5.11, and 5.36 ppm and three N-acetyl groups at δ 2.04-2.06 ppm. Therefore, the oligosaccharide contained all components of the polysaccharide, except for ethanolamine phosphate.

The ^{1}H- and ^{13}C-NMR chemicals shift data of the oligosaccharide are summarized in Tables 1 and 2. Based on the $J_{H,H}$ coupling constant values, three spin systems were assigned to α-Glc*p*NAc, α-Gal*p*NAc, and β-Gal*p*NAc, and the fourth spin system belonged to ribitol. The configurations of the glycosidic linkages were confirmed by a ROESY experiment, which revealed intraresidue H1/H3,H5 correlations that are typical of β-linked pyranosides, only for Gal*p*NAc.

A low-field displacement of the signals for C3 of Glc*p*NAc to δ 78.0 (+6.3 ppm), C4 of α-Gal*p*NAc to δ 76.5 (+8.1 ppm), and C2 of Rib-ol to δ 80.8 (+ 7.3 ppm) defined the modes of glycosylation. The ROESY spectrum showed the following correlations between the transglycosidic protons: β-Gal*p*NAc H1/α-Gal*p*NAc H4 at δ 4.69/4.18 ppm, α-Gal*p*NAc H1/Glc*p*NAc H3 at δ 5.36/3.89 ppm, and Glc*p*NAc H1/Rib-ol H2 at δ 5.11/3.96 ppm. These data confirmed the substitution pattern and revealed the following structure of the oligosaccharide:

β-D-Gal*p*NAc-(1→4)-α-D-Gal*p*NAc-(1→3)-

α-D-Glc*p*NAc-(1→2)-D-Rib-ol.

The ^{31}P-NMR spectrum of the initial polysaccharide contained signals for two phosphate groups at δ 2.71 and 2.96 ppm. The minor series of signals in the ^{1}H- and ^{13}C-NMR spectra (Tables 1 and 2) resembled much the spectra of the oligosaccharide. The major series was distinguished by the presence of the signals for ethanolamine phosphate at δ_H 3.29 and 4.14 ppm, δ_C 41.3 and 63.1 ppm for CH_2N- and CH_2O-groups, respectively. In the ^{1}H,^{31}P HMQC spectrum, the CH_2O-signal correlated with the ^{31}P-NMR signal at δ 4.14/2.71 ppm. These data

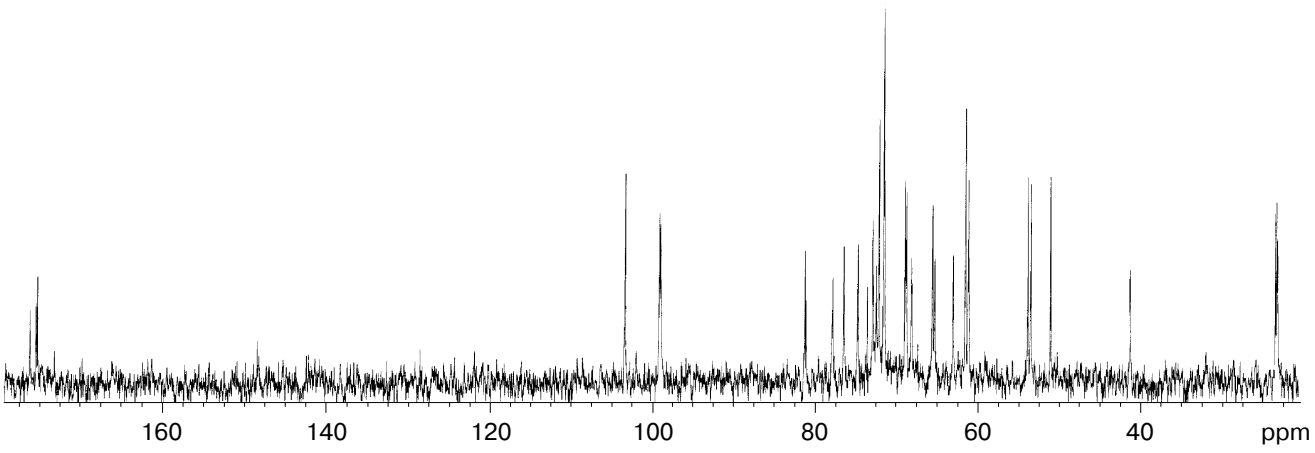

Fig. 5. ^{13}C-NMR spectrum of the O-specific polysaccharide of *P. mirabilis* O16.

suggested that the major repeating unit contains Etn-*P*, which is absent from the minor repeating unit.

The most significant differences between the ^{13}C-NMR spectra of the polysaccharide (major series) and the oligosaccharide were observed for the signals for C6 of Glc*p*NAc (δ 65.3 versus 61.6 ppm), C6 of β-Gal*p*NAc (δ 65.6 versus 62.3 ppm), and C5 of ribitol (δ 68.2 versus 64.1 ppm, respectively). All these and the neighboring carbon signals in the polysaccharide were split due to coupling to phosphorus. The $^{1}H,^{31}P$ HMQC spectrum showed cross-peaks for the ^{31}P-NMR signal of Etn-*P* with the Glc*p*NAc H6a,H6b signals at δ 2.71/4.12 and 2.71/4.18 ppm. The other ^{31}P-NMR signal at δ 2.96 ppm gave cross-peaks with Rib-ol H5a,H5b at δ 3.97 and 4.06 ppm. These data suggested that Etn-*P* is attached at position 6 of Glc*p*NAc, whereas the other phosphate group 5→6-interlinks ribitol and β-Gal*p*NAc.

On the basis of the data obtained, it was concluded that the O-specific polysaccharide of *P. mirabilis* O16 has the structure shown in Table 3. In the article on the structure of this polysaccharide that was published earlier [15], a wrong configuration was assigned to the ribitol residue.

DISCUSSION

A number of *Proteus* O-specific polysaccharides contain phosphoric acid residues occurring as noncyclic diesters. These phosphorylated polysaccharides can be divided into the following three types.

1. Polysaccharides that contain a non-sugar substituent linked to the main chain via a phosphate group. The non-sugar group may be glycerol, D-ribitol, 2-aminoethanol (ethanolamine), and 2-[(R)-1-carboxyethylamino]ethanol [3]. The most common from them is ethanolamine phosphate, which has been found in many polysaccharides, including all polysaccharides studied in this work (Table 3), and can be considered as a typical component of *Proteus* O-antigens. It often occurs in a non-stoichiometric amount like, e.g., in the polysaccharides of *P. vulgaris* O17, *P. mirabilis* O16 and O33 (Table 3). In contrast, glycerol phosphate [16] and ribitol phosphate [17] have been found in only one polysaccharide each. The latter has been reported for the first time as a component of bacterial polysaccharide in a non-classified *P. mirabilis* strain, D52, whose partial structure was established in 1970s [17]. Later, this strain was included into *Proteus* serogroup O33 [18], and the O-specific polysaccharide structure of *P. mirabilis* D52 was found to be identical to that of *P. mirabilis* O33 established in this work (Table 3).

2. Polysaccharides that include an alditol phosphate in the main polysaccharide chain. They resemble teichoic acids of Gram-positive bacteria and are uncommon among O-antigens of Gram-positive bacteria. Previously, only glycerol has been reported as alditol [19], whereas the two known *Proteus* polysaccharides with ribitol, those of *P. mirabilis* O16 and *P. penneri* 103, were described for the first time in this work (Table 3). Both these polysaccharides, as well as the polysaccharide of *P. mirabilis* O33 contain D-ribitol residues phosphorylated at position 5.

3. Polysaccharides in which oligosaccharide repeating units are connected by phosphate groups. They differ from the polysaccharides discussed above by the absence of alditol. Polymers of this type have been previously reported in the lipopolysaccharides of *P. vulgaris* O1 (OX19) [20], O21 [21], and *P. mirabilis* O48 [22].

Noteworthy, the most phosphorylated *Proteus* polysaccharides include multiple negatively and positively charged groups. The most typical combination of such groups is phosphoric acid and ethanolamine. In some other *Proteus* lipopolysaccharides, multiple charges are provided by amides of D-galacturonic or D-glucuronic acid with L-lysine or N^{ε}-[(R)-1-carboxyethyl]-L-lysine [3]. A high concentration of charged groups on the surface polysaccharides may help adaptation of *Proteus* cells to growing under different pH and may promote formation of stones in the urinary tract.

The structures of the ribitol phosphate-containing polysaccharides studied in this work are unique among the structures of *Proteus* O-antigens. This finding is in agreement with serological classification of *P. mirabilis* O16 and O33 in separate O-serogroups and showed that *P. penneri* strain 103 should be placed in a new *Proteus* O-serogroup too. In contrast, two other polysaccharides studied, those from *P. penneri* 31 and *P. vulgaris* O17, demonstrated a marked structural similarity to other *Proteus* O-antigens studied earlier. The structures of the related polysaccharides of *P. vulgaris* O19, *P. penneri* 63, and *P. penneri* 16 are shown in Table 3.

The polysaccharide of *P. penneri* 31 has the same structure of the linear repeating unit as one of the non-phosphorylated polysaccharides of *P. vulgaris* O19, namely that of strain CNCTC 4349 [22], which differs only in the absence of ethanolamine phosphate. Similarly, the polysaccharide of *P. penneri* 16 [13] has the same main chain as that of *P. vulgaris* O17. It differs not only in the absence of ethanolamine phosphate, but also in the presence of a glucose monosaccharide side chain. The two pairs of the O-antigens were found to be serologically related as well (authors' unpublished data) and, therefore, we propose to place *P. penneri* strains 16 and 31 into *Proteus* serogroups O17 and O19, respectively, as subgroups.

In addition, the polysaccharide of *P. penneri* 31 shares some structural features with the polysaccharide of *P. penneri* 63 [23], both containing a phosphorylated L-Fuc*p*NAc-(1→3)-β-D-Glc*p*NAc6*P*Etn disaccharide fragment (Table 3). However, no serological relationship was observed between these O-antigens (authors' unpublished data), and, therefore, *P. penneri* strain 63 was classified into a separate serogroup O68 [23].

To summarize, the results of our chemical studies of the O-specific polysaccharides enabled improvement of the classification of *Proteus*, which is important for epidemiological purposes. Further immunochemical studies should result in the creation of the full, chemically substantiated classification of bacterial strains of this genus.

This work was supported by grant 99-04-48279 of the Russian Foundation for Basic Research and grant 6 PO4A 074 20 of the Science Research Committee (KBN, Poland).

REFERENCES

1. Larsson, P. (1984) *Meth. Microbiol.*, **14**, 187-214.
2. Penner, J. L., and Hennessy, C. (1980) *J. Clin. Microbiol.*, **12**, 304-309.
3. Knirel, Y. A., Kaca, W., Rozalski, A., and Sidorczyk, Z. (1999) *Polish J. Chem.*, **73**, 895-907.
4. Zych, K., Kowalczyk, M., Knirel, Y. A., and Sidorczyk, Z. (2000) *Adv. Exp. Med. Biol.*, **485**, 339-344.
5. Westphal, O., and Jann, K. (1965) *Meth. Carbohydr. Chem.*, **5**, 83-91.
6. Hanniffy, O., Shashkov, A. S., Senchenkova, S. N., Tomshich, S. V., Komandrova, N. A., Romanenko, L. A., Knirel, Y. A., and Savage, A. V. (1999) *Carbohydr. Res.*, **321**, 132-138.
7. Bock, K., and Pedersen, C. (1983) *Adv. Carbohydr. Chem. Biochem.*, **41**, 27-66.
8. Lipkind, G. M., Shashkov, A. S., Knirel, Y. A., Vinogradov, E. V., and Kochetkov, N. K. (1988) *Carbohydr. Res.*, **175**, 59-75.
9. Jansson, P.-E., Kenne, L., and Widmalm, G. (1989) *Carbohydr. Res.*, **188**, 169-191.
10. Sawardeker, J. S., Sloneker, J. H., and Jeanes, A. (1965) *Analyt. Chem.*, **37**, 1602-1603.
11. Leontein, K., Lindberg, B., and Lönngren, J. (1978) *Carbohydr. Res.*, **62**, 359-362.
12. Rundlöf, T., and Widmalm, G. (1996) *Analyt. Biochem.*, **243**, 228-233.
13. Vinogradov, E. V., Sidorczyk, Z., Swierzko, A., Rozalski, A., Daeva, E. D., Shashkov, A. S., Knirel, Y. A., and Kochetkov, N. K. (1991) *Eur. J. Biochem.*, **197**, 93-103.
14. Shashkov, A. S., Lipkind, G. M., Knirel, Y. A., and Kochetkov, N. K. (1988) *Magn. Reson. Chem.*, **26**, 735-747.
15. Toukach, F. V., Arbatsky, N. P., Shashkov, A. S., Knirel, Y. A., Zych, K., and Sidorczyk, Z. (2001) *Carbohydr. Res.*, **331**, 213-218.
16. Uhrín, D., Brisson, J.-R., MacLean, L. L., Richards, J. C., and Perry, M. B. (1994) *J. Biomolec. NMR*, **4**, 615-630.
17. Gmeiner, J. (1977) *Eur. J. Biochem.*, **74**, 171-180.
18. Zych, K., Toukach, F. V., Arbatsky, N. P., Kolodziejska, K., Senchenkova, S. N., Shashkov, A. S., Knirel, Y. A., and Sidorczyk, Z. (2001) *Eur. J. Biochem.*, **268**, 4346-4351.
19. Perepelov, A. V., Torzewska, A., Shashkov, A. S., Senchenkova, S. N., Rozalski, A., and Knirel, Y. A. (2000) *Eur. J. Biochem.*, **267**, 788-793.
20. Ziolkowski, A., Shashkov, A. S., Swierzko, A., Senchenkova, S. N., Toukach, F. V., Cedzynski, M., Amano, K.-I., Kaca, W., and Knirel, Y. A. (1997) *FEBS Lett.*, **411**, 221-224.
21. Bartodziejska, B., Toukach, F. V., Vinogradov, E. V., Senchenkova, S. N., Shashkov, A. S., Ziolkowski, A., Czaja, J., Perry, M. B., Knirel, Y. A., and Rozalski, A. (2000) *Eur. J. Biochem.*, **267**, 6888-6896.
22. Vinogradov, E. V., Kaca, W., Knirel, Y. A., Rozalski, A., and Kochetkov, N. K. (1989) *Eur. J. Biochem.*, **180**, 95-99.
23. Shashkov, A. S., Kondakova, A. N., Senchenkova, S. N., Zych, K., Toukach, F. V., Knirel, Y. A., and Sidorczyk, Z. (2000) *Eur. J. Biochem.*, **267**, 601-605.